Chinese Chemical Letters 35 (2024) 109221

Contents lists available at ScienceDirect

Chinese Chemical Letters

journal homepage: www.elsevier.com/locate/cclet

Double active sites promoting hydrogen evolution activity and stability of $CoRuOH/Co_2P$ by rapid hydrolysis

Bin Dong*, Ning Yu, Qiu-Yue Wang, Jing-Ke Ren, Xin-Yu Zhang, Zhi-Jie Zhang, Ruo-Yao Fan, Da-Peng Liu, Yong-Ming Chai*

State Key Laboratory of Heavy Oil Processing, College of Chemistry and Chemical Engineering, China University of Petroleum (East China), Qingdao 266580, China

ARTICLE INFO

Article history:
Received 15 January 2023
Revised 25 September 2023
Accepted 17 October 2023
Available online 24 October 2023

Keywords:
$CoRuOH/Co_2P/CF$
Enhanced activity and stability
Double active site
Large current density
Hydrogen evolution reaction

ABSTRACT

Cobalt-based phosphides show excellent hydrogen evolution reaction (HER) performance, however, improving the intrinsic activity and stability of it in alkaline electrolyte still remains a challenge. Herein, $CoRuOH/Co_2P/CF$ with heterojunction structure was developed by means of molten salt and rapid hydrolysis (30 s). The OH^- from rapid surface hydrolysis of Co_2P as a hydrogen adsorption site can facilitate the formation of thin CoRuOH layer as a water dissociation site, which may bring out better synergistic effect for alkaline HER. Moreover, the covering of CoRuOH can improve the stability of Co_2P for HER. When drives at 100 mA/cm^2, it only requires overpotential of 81 mV in 1.0 mol/L KOH (25 °C). Even at higher current density (1000 mA/cm^2), $CoRuOH/Co_2P/CF$ can also operate stability for at least 100 h. When coupling with NiFe-LDH/IF in a two-electrode system, the voltage of NiFe-LDH/$IF^{(+)}$ || $CoRuOH/Co_2P/CF^{(-)}$ at 1000 mA/cm^2 is merely 1.77 V with 100 h, demonstrating great potential for water splitting. The implementation of this work provides a new strategy and reference for the further improvement of transition metal phosphides as HER electrocatalysts.

The over-utilization of traditional fossil resources led to serious energy, environmental and health problems. Therefore, it is necessary to develop a clean, friendly and green renewable energy system in the future [1,2]. Hydrogen is considered to be a great supplement or alternative to fossil fuels because of zero-carbon emission and high calorific value [3,4]. However, the current hydrogen production relies more on coal, natural gas and methane, which has a large number of carbon emissions in the cycle process. Water electrolysis has been recognized as a sustainable way for producing high-purity H_2, which can be generated through electrochemical hydrogen evolution reaction (HER) driven by renewable energy without any harmful pollution. It is very important to develop electrocatalysts with high activity and stability to improve the efficiency of hydrogen evolution [5–8]. Precious metal Pt-based catalytic materials are regarded as the most advanced electrocatalysts due to their empty d orbital, which shows appropriate effects on the H adsorption intermediates [9,10]. However, the high cost and scarcity of them inhibit their widespread application. Therefore, the development of alternative non-noble metal HER catalysts becomes challengeable [11,12].

From the perspective of application, hydrogen production requires large-scale production at a high current density (at least 400 mA/cm^2), which requires sufficient mechanical stability and activity of the catalyst [13,14]. However, most reported catalysts operate at 10 mA/cm^2, even though they can maintain stability for tens or tens of h [15–17]. Under the large-current working condition of water electrolyzes, the catalyst should conform to the following points as far as possible. First, higher intrinsic activity to reduce energy consumption. Second, it has strong corrosion resistance in alkaline electrolyte. Third, strong mechanical properties to prevent the active site from falling off. Four, self-supported and three-dimensional catalysts to facilitate rapid diffusion of reactants and gas removal. Fourth, higher soil abundance and lower preparation cost [18–21].

Generally, the transition metal phosphate (TMP) has been intensively investigated as a promising candidate for HER electrocatalyst, which can be grown directly on collectors (such as nickel foam, cobalt foam, and carbon cloth) by hydrothermal method, thereby improving the overall catalytic effect [22,23]. Among the various developed electrocatalysts, the cobalt phosphide shows promising HER properties due to its optimized hy-

* Corresponding authors.
E-mail addresses: dongbin@upc.edu.cn (B. Dong), ymchai@upc.edu.cn (Y.-M. Chai).

https://doi.org/10.1016/j.cclet.2023.109221
1001-8417/

drogen adsorption-desorption effect [24]. Where the negatively charged phosphorus can easily trapping the positively charged protons. However, this high activity of hydrogen evolution cannot be maintained for a long time because the surface metals are easily oxidized. The metal phosphorus oxides formed on the surface of cobalt phosphide will eventually lead to a decrease HER activity. Therefore, the long-term operation of cobalt phosphide under high HER activity becomes very challenging.

Currently, the most recognized mechanism for alkaline HER is the Volmer-Heyrovsky process. Where the Volmer refers to $H_2O + e^- \rightarrow H_{ads} + OH^-$ (dissociation of water molecular) that has been regarded as the rate-limiting step to rapidly produce the adsorbed hydrogen intermediates (H_{ads}). Accelerating the hydrolysis dissociation step in alkaline environment can greatly improve the intrinsic catalyst activity [25,26]. For example, our group has earlier explored doping phosphorus atoms onto iron foam-supported Fe_3O_4 through low temperature phosphorylation, where Fe_3O_4 served as the hydrolysis dissociation site [27]. Relevant studies suggest that the metal hydroxide will inevitably be generated on the surface of phosphide due to the adsorption of OH^- in an alkaline environment, which can be used as the active site to accelerate the Volmer steps in HER [25–29]. However, the amount of metal hydroxide grown in this way is not sufficient to cover the entire material. During the process of hydrogen production test, the phosphorus loss in metal phosphide is serious, which further affects HER activity of it [25,30]. It is possible to solve the above problems by rapid hydrolysis of weak acid ions to form a thin layer of hydroxide. In special, the phosphide will dissolve weakly and produce a small amount of P anion a hot solution, which can react rapidly with the water molecule and produce a corresponding amount of OH^- [31–33]. When meeting the extra metal cation in solution, they will precipitate and finally grow on the surface of catalyst. Compared with our previous work, the same metal-oxygen bond was constructed as the hydrolysis dissociation point, the formed metal hydroxide on the surface of metal phosphates could not only build hydrolytic sites to promote hydrogen evolution efficiency, but also act as a protective layer to inhibit the loss of P. However, this novel idea has not been tried, and the details still need to be explored.

To this end, we have developed a new strategy of rapid hydrolysis combined with molten salt to synthesize the cobalt-ruthenium hydroxide coated cobalt phosphide catalyst on cobalt foam (CoRuOH/Co_2P/CF). Attributed to the double active sites (water dissociation and H adsorption/recombination), the prepared CoRuOH/Co_2P/CF shows higher HER activity and stability compared with pure Co_2P/CF, which merely requires an ultralow overpotential of 81 mV to acquire 100 mA/cm^2 in 1 mol/L KOH electrolyte. Even at a higher current density of 1000 A/cm^2, it can also operate stably for 100 h. When coupled with NiFe-LDH/IF as the anode in an overall water splitting alkaline electrolyzer, it only needs a cell voltage of 1.77 V to drive 1000 mA/cm^2 and can continuously work for 100 h at 1000 mA/cm^2. The excellent electrolytic water performance of CoRuOH/Co_2P/CF enables it a great potential for hydrogen production in the future.

As illustrated in Scheme 1, the CoRuOH/Co_2P/CF catalyst was synthesized by a facile two-step process. Firstly, the precursors of $CoNO_3OH$/CF and Co_2P were prepared by means of molten salt and phosphating reaction. Subsequently, the CoRuOH loaded on the substrate of Co_2P/CF was quickly prepared by the method of hydrolysis. Where the hydrolysis power mainly came from the reaction of cobalt phosphide with water molecules. At high temperature (100 °C), negatively valued P ions could react with water and thus producing amount of OH^-, which made the surface of the catalyst appear weakly alkaline. When additional Ru^{3+} and Co^{2+} in the solution meted with them, thin nanosheets with smaller K_{sp} value will were produced rapidly. The formation of CoFeOH can promote to generate the highly active phase of amorphous-crystalline interface. CoRuOH is cobalt-ruthenium hydroxide which represents a mixture of cobalt hydroxide and ruthenium hydroxide. The relevant expression can be expressed as follows (Eqs. 1–3):

$$P^{3-} + 4H_2O \rightarrow PH^{4+} + 4OH^- \quad (1)$$

$$Ru^{3+} + 3OH^- \rightarrow Ru(OH)_3 \quad (2)$$

$$Co^{2+} + 2OH^- \rightarrow Co(OH)_2 \quad (3)$$

The phase structure of the samples was first analyzed by an X-ray diffractometer (XRD). As displayed in Fig. S1a (Supporting information), the characteristic peaks for cobalt precursor could be assigned to $CoNO_3OH$ (No. 00-048-0492). After phosphating process, the $CoNO_3OH$ has transformed into the Co_2P with PDF card of No. 00-054-0413 (Fig. 1a). It was important to note that the hydrolysis treatment had little change on the crystal structure of Co_2P, indicating that the cobalt-ruthenium hydroxide (Fig. 1a) or ruthenium hydroxide (Fig. S1b in Supporting information) that was produced was in an amorphous condition. Moreover, the X-ray photoelectron spectroscopy (XPS) was applied to compare the elemental valence of the samples. As depicted in Fig. 1b, the characteristic peak of Ru in survey spectra was only observed in CoRuOH/Co_2P/CF, implying a successful joining of Ru in it. The deconvolution peak of Co 2p is used to further examine the valence distribution of Co (Fig. 1c). The spectrum exhibits two sets of spin-orbital doublets corresponding to Co $2p_{3/2}$ and Co $2p_{1/2}$ with satellite peaks. In Co 2p XPS spectra for Co_2P/CF, the peaks at 778.5 and 793.4 eV were attributed to the species of Co^{3+}. While the peaks located at 781.7 and 791.7 eV belong to the Co^{2+}, indicating the presence of the Co-P and Co-OH species. The binding energies of Co species in CoRuOH/Co_2P/CF are roughly 0.4 eV higher than that of Co_2P/CF, which might be the result of neutralization of Co_2P with newly formed cobalt hydroxide [34–36]. The recorded

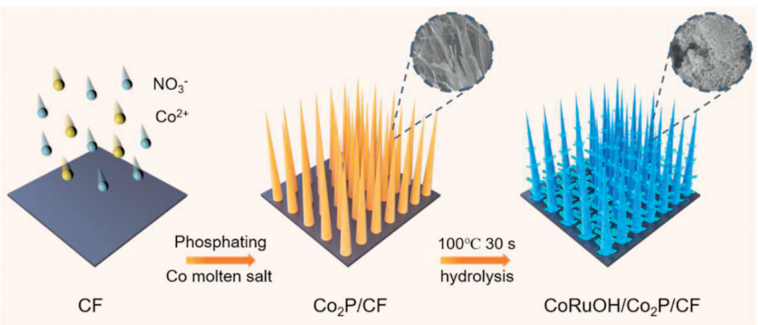

Scheme 1. Schematic diagram of the CoRuOH/Co_2P/CF synthesis process.

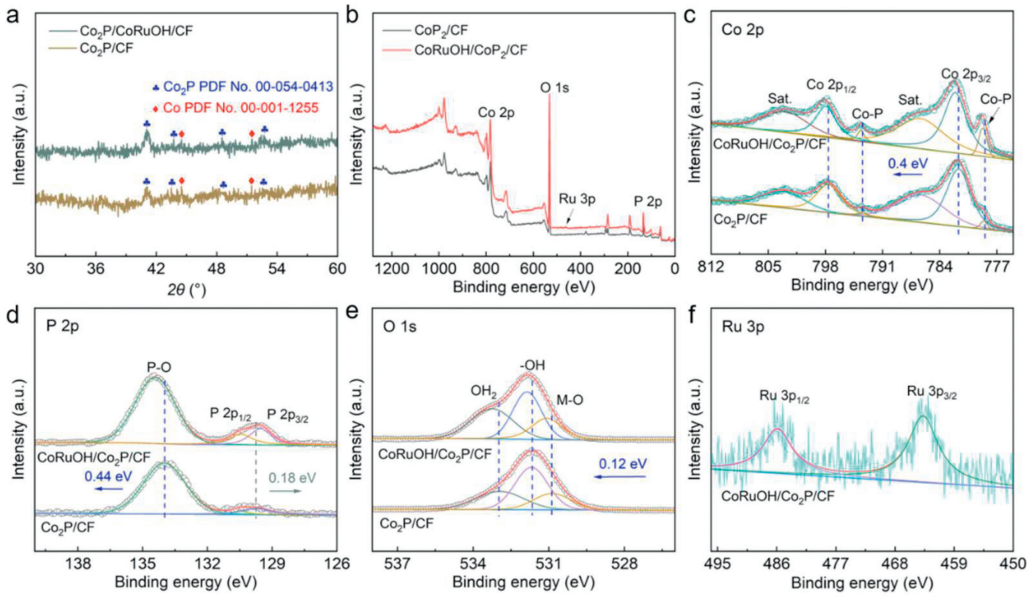

Fig. 1. (a) XRD patterns of Co_2P/CF and CoRuOH/Co_2P/CF. (b) XPS survey spectra of Co_2P/CF and CoRuOH/Co_2P/CF. Comparison of (c) Co 2p, (d) P 2p and (e) O 1s binding energy between the Co_2P/CF and CoRuOH/Co_2P/CF. (f) High-resolution XPS spectrum of Ru 3p for the CoRuOH/Co_2P/CF.

spectra P 2p (Co_2P/CF) can be fitted into three peaks, where the two peaks located at about 129.8 eV and 130.5 eV come from P $2p_{3/2}$ and P $2p_{1/2}$ of the bind of P-M, while the peak at 133.9 eV is form P-O species owing to the inevitable oxidation of surface metal phosphates by air (Fig. 1d). Slimily, the peaks position of P-M in CoRuOH/Co_2P/CF has decreased dramatically about 0.18 eV after the hydrolysis, indicating an increase of electrons on its surface, which was consistent with the valence state change of cobalt [25,37]. The O 1s spectra can be subdivided into three peaks. The three peaks at 530.8, 531.6 and 532.9 eV represent O-M, O-H and H_2O. There are associated with *meta*-oxygen bonds in the metal oxide, the hydroxyl-like groups in the material, and the multiplicity of water molecules, respectively (Fig. 1e) [38]. The Ru 3p spectrum in CoRuOH/Co_2P/CF was shown in Fig. 1f. The trivalent state of Ru in the generated hydroxide was demonstrated by the peaks at 463.48 and 485.8 eV, which were the Ru $3p_{3/2}$ and Ru $3p_{1/2}$ [39,40].

The morphology of all samples was characterized by scanning electron microscopy (SEM) and transmission electron microscopy (TEM). As shown, SEM image of $CoNO_3OH$/CF in Fig. 2a clearly visualized a smooth nanowire. After phosphating process, the as-prepared Co_2P became rough and the structure of nanoroad still be maintained (Fig. S2 in Supporting information). However, it could be seen from Figs. 2b and c that there were a large number of nanosheet structures generated on the surface of Co_2P, which might be the result of rapid hydrolysis of phosphorus anions at high temperature. Similarly, SEM of RuOH/Co_2P/CF (Fig. S3 in Supporting information) and CoOH/Co_2P/CF (Fig. S4 in Supporting information) maintain good nanorod morphology except that the morphology of nanosheets was sparse and has not the tendency of cross-linking growth. This phenomenon could be evident from the HRTEM images in Figs. 2d–f. Where the Co_2P with distinct crystal structure was encapsulated by the CoRuOH nanosheets and finally disclosed a core-shell structure, which was consistent with the above SEM results (Figs. 2b and c). Cobalt-ruthenium hydroxide is further demonstrated to be in an amorphous state by the lack of clear lattice stripes in HRTEM for the loose nanosheet structure. Particularly, the CoRuOH shell had a thickness of 30–50 nm, which not only reduced phosphorus loss but also created a new dissociation active site, accelerating the evolution of hydrogen. The loose

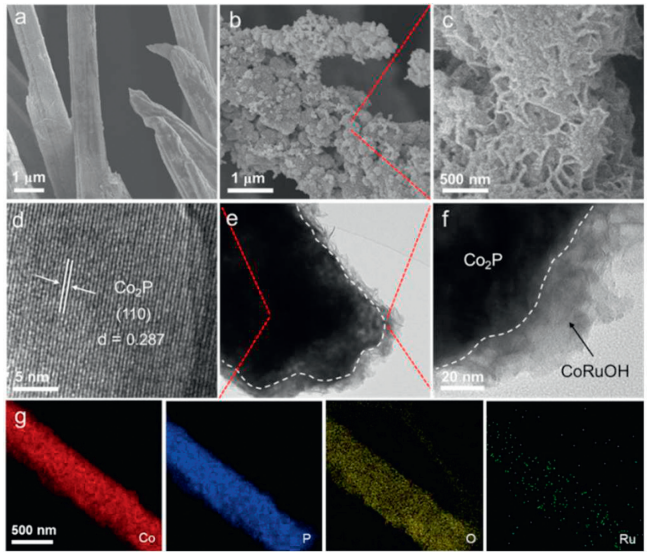

Fig. 2. SEM images of (a) $CoNO_3OH$/CF and (b, c) CoRuOH/Co_2P/CF. (d) HRTEM and (e, f) TEM images of the CoRuOH/Co_2P/CF. (g) The energy dispersive X-ray (EDX) mappings images of the CoRuOH/Co_2P/CF for Co, P, O and Ru.

nanosheet structure of CoRuOH has a large number of pores and has a certain degree of flexibility to cover the Co_2P surface (Fig. S5 in Supporting information). This special structure is conducive to the rapid overflow of bubbles generated on the electrode surface during the electrolytic process, preventing a large number of bubbles from obstructing the contact between the electrocatalyst and the electrolyte. If the hydrolysis time is too long, thicker cobalt-ruthenium hydroxide may be formed, thus covering up Co_2P. Additionally, the energy dispersive X-ray (EDX) mappings were presented in Fig. 2g, revealing a homogeneous distribution of Co, P, O and Ru elements in the as-synthesized CoRuOH/Co_2P/CF electrocatalyst.

HER performance of CoRuOH/Co_2P/CF and contrast samples, including bare cobalt foam (CF), Co Pre/CF, Co_2P/CF and RuOH/Co_2P/CF were tested by linear sweep voltammograms

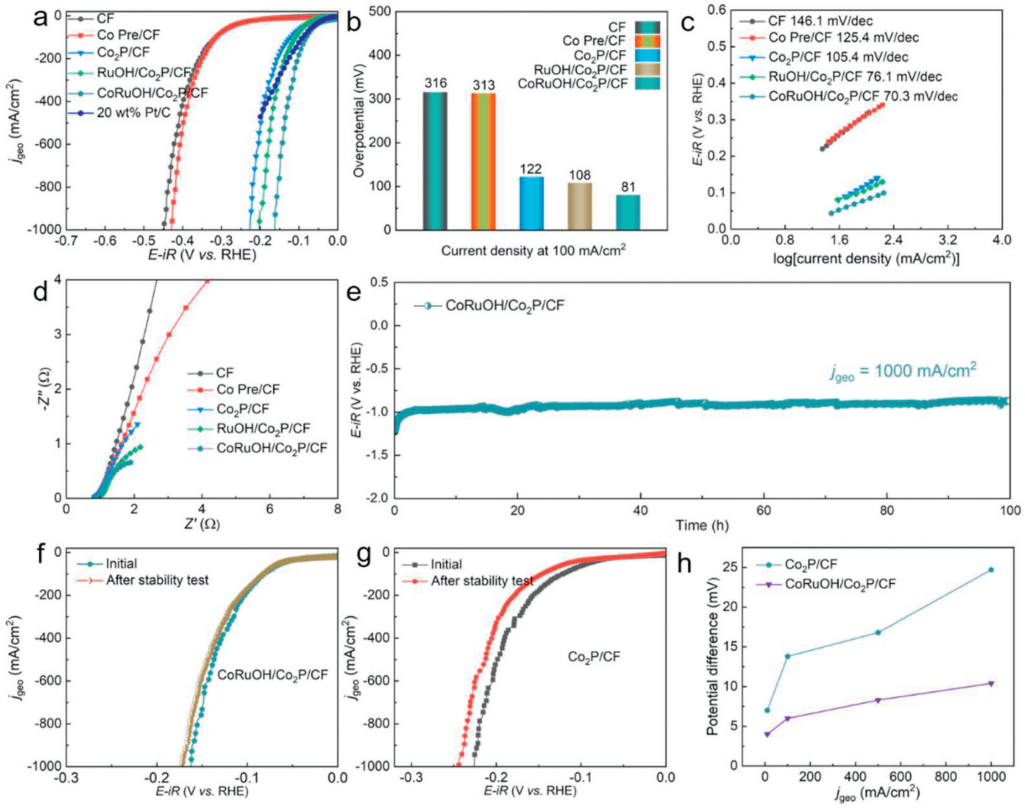

Fig. 3. Electrochemical tests: (a) HER polarization curves, (b) over-potentials at current density of 100 mA/cm^2, (c) Tafel plots, (d) Nyquist plots and (e) stability tests of CoRuOH/Co_2P/CF at 1000 mA/cm^2 for 100 h. LSV curves of (f) CoRuOH/Co_2P/CF and (g) Co_2P/CF recorded before and after stability tests. (h) Overpotential difference of Co_2P/CF and CoRuOH/Co_2P/CF before and after stability tests.

(LSV) with iR-compensation in 1 mol/L KOH alkaline electrolyte. Figs. 3a–c were the polarization curves, overpotentials and Tafel plots of catalysts. Where the pure CF and Co Pre/CF displayed an inferior HER performance. When treated with sodium hypophosphite at 350 °C, the obtained Co_2P/CF showed a Tafel slope of 105.4 mV/dec and an overpotential of 122 mV at the current density of 100 mA/cm^2. The RuOH/Co_2P/CF showed an overpotential of 108 mV at 100 mA/cm^2 and a Tafel slope of 76.1 mV/dec. The CoRuOH/Co_2P/CF yielded a lower overpotential (81 mV) at 100 mA/cm^2 and Tafel slope (70.3 mV/dec), which was comparable to the state-of-art commercial Pt/C and other HER catalysts (Table S1 in Supporting information). The observation indicates that introduction of CoRuOH indeed accelerates water dissociation and reduces overpotentials. The highest HER activity of CoRuOH/Co_2P/CF might be attributed to its double active sites. Cobalt phosphide might be used as a fantastic site for the adsorption and desorption of hydrogen, whereas ruthenium-cobalt hydroxide could facilitate the rapid dissociation of water molecules [41–45]. Since the Tafel slope of CoRuOH/Co_2P/CF was higher than 40 mV/dec, the electrocatalytic HER kinetics was decided by Heyrovsky step. The CoRuOH layer is introduced on the Co_2P surface by hydrolysis of P, which is considered to be the active site of the Volmer reaction. This rapid hydrolysis method enables CoRuOH to bind closely to the interior of Co_2P as the active site of Heyrovsky reaction, forming an obvious amorphous-crystallization interface. The double layer capacitance (C_{dl}) was estimated because it is positively correlated with the electrochemically active surface area (ECSA) of the catalyst. The C_{dl} of CoRuOH/Co_2P/CF (45.8 mF/cm^2) is greater than Co_2P/CF (28.4 mF/cm^2), indicating that the CoRuOH formed by rapid hydrolysis increases the ECSA. The corresponding ECSA was calculated as shown in the Table S2 (Supporting information). Fig. 3d were the Nyquist plots of all samples obtained by the measurement of electrochemical impedance spectroscopy (EIS). The size of the semicircle in the Nyquist diagram indicated the resistance of the catalyst material to charge. As displayed, CoRuOH/Co_2P/CF electrode has the lowest charge transfer resistance compared with other reference catalysts, which means the fastest electron transfer in HER process. The electrochemical durability was another important indicator for catalyst. Therefore, the stability of CoRuOH/Co_2P/CF was tested by chronoamperometry curves for 100 h in 1 mol/L KOH (25 °C). Fig. 3e revealed that the CoRuOH/Co_2P/CF could run for a long time at large current density (1000 mA/cm^2) while the catalytic activity remained basically unchanged. Furthermore, the polarization curves of CoRuOH/Co_2P/CF before and after 10 h stability were compared. We found that after testing, HER activity decreased slightly after test due to loss or oxidation of phosphide during operation, but still maintained high activity (Fig. 3f). This indicates that CoRuOH located on the surface of Co_2P can effectively reduce the loss of P species, thus maintaining the activity in the long-term stability test. In addition, CoRuOH has a soft two-dimensional sheet structure and a self-supporting three-dimensional skeleton structure, which promotes the rapid transmission of ions in the electrolyte and the elimination of produced bubbles. However, the activity of pure Co_2P/CF decreased significantly after the same test, indicating that the coating of cobalt-ruthenium hydroxide contributed to the improvement of the stability of the catalyst (Figs. 3g and h). In summary, the rapid hydrolysis method to form cobalt-ruthenium hydroxide on the surface of Co_2P/CF not only provides more water dissociation site to enhance the activity of HER, but also effectively reduces the loss of P to maintain HER for a long time.

Motivated by the excellent HER performance of CoRuOH/Co_2P/CF, a two-electrode electrolyzer in 1.0 mol/L KOH was assembled by using CoRuOH/Co_2P/CF as cathode and NiFe-

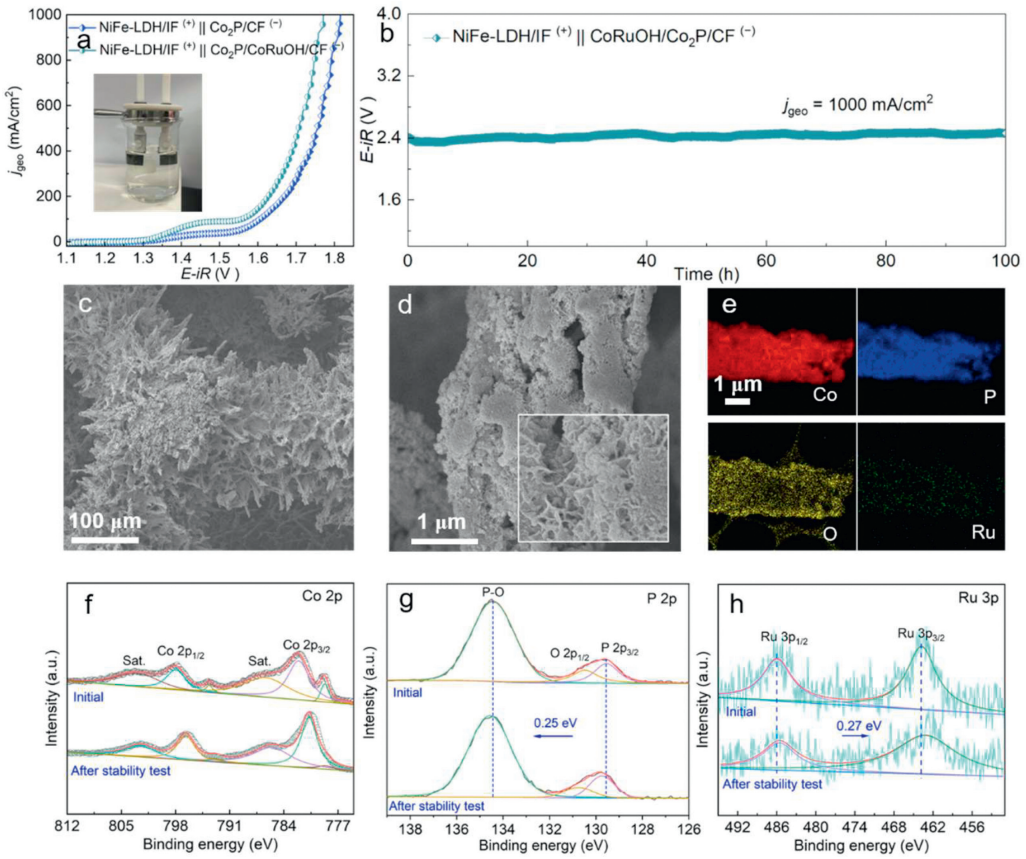

Fig. 4. Overall catalytic water splitting activities of NiFe-LDH/IF$^{(+)}$ || Co_2P/CF$^{(-)}$ and NiFe-LDH/IF$^{(+)}$ || CoRuOH/Co_2P/CF$^{(-)}$ in 1 mol/L KOH. (a) Polarization curves with iR correction. Inset: Practical device of water splitting. (b) Stability curve tested at a constant current of 100 mA/cm^2 without iR correction. (c, d) SEM and (e) EDX elemental mapping images of CoRuOH/Co_2P/CF after stability test. High-resolution XPS spectra of (f) Co 2p, (g) P 2p and (h) Ru 3p after stability test.

LDH/IF (Fig. S7 in Supporting information) as anode for overall water splitting (named as NiFe-LDH/IF$^{(+)}$ || CoRuOH/Co_2P/CF$^{(-)}$) [46–48]. By contrast, the couple of NiFe-LDH/IF$^{(+)}$ || Co_2P/CF$^{(-)}$ has also been assembled. As shown in Fig. 4a, the polarization curves of the NiFe-LDH/IF$^{(+)}$ || CoRuOH/Co_2P/CF$^{(-)}$ needed a voltage of 1.77 V to achieved the current density of 1000 mA/cm^2, which was much lower than the NiFe-LDH/IF$^{(+)}$ || Co_2P/CF$^{(-)}$ cell (1.82 V). This phenomenon once again demonstrated the importance of growing cobalt-ruthenium hydroxides for Co_2P. From an application point, the stability of the electrolyzer over long periods of time at high current densities was also considered. And Fig. 4b was the chronopotentiometric curves recorded at 1000 mA/cm^2 in 1 mol/L KOH solution. Where the NiFe-LDH/IF$^{(+)}$ || CoRuOH/Co_2P/CF$^{(-)}$ cell could be tolerated for 100 h with a negligible voltage fluctuation, reflecting the huge application potential of this catalytic system. The SEM and XPS were applied to characterize the CoRuOH/Co_2P/CF catalyst after stability test for further exploring the changes in structure and chemical states. As shown in Figs. 4c and d, the CoRuOH/Co_2P/CF still existed in the form of nanowire and the cobalt-ruthenium hydroxide was still in the state of nanosheet after the long period of hydrogen precipitation, implying the excellent mechanical stability of it. In addition, the above phenomenon could also be reflected in the EDX elemental mapping (Fig. 4e), where the elements of Co, P, O and Ru still presented a high degree of dispersion in the catalyst. The XPS survey spectra of CoRuOH/Co_2P/CF before and after the stability test were shown in Fig. S8a (Supporting information). And the Co, P, O and Ru elements could be clearly observed in it. After the long-term stability test of CoRuOH/Co_2P/CF, the XPS spectra in the Co 2p region showed a peak shift of 1.2 eV towards low energy, indicating that a new hydroxide (such as cobalt hydroxide) may be formed (Fig. 4f). For P, O and Ru elements, the binding energy was shifted to different degrees, which might be caused by local phosphorus loss and new hydroxide formation during the HER process (Figs. 4g, h and Fig. S8b in Supporting information). But for species, it has not changed significantly, which was consistent with the results of SEM (Figs. 4c and d) and EDX data (Fig. 4e). The above analysis suggested that catalyst of CoRuOH/Co_2P/CF can be used as an excellent catalyst for hydrogen evolution for future large-scale production of hydrogen. And the high HER performance may be attributed to the following points: (1) The preparation method of molten salt makes the surface of cobalt foam possess abundant hydrogen adsorption-desorption active sites (Co_2P). (2) The introduction of cobalt-ruthenium hydroxide by rapid hydrolysis contributes to the dissociation of water molecules during HER. (3) The three-dimensional framework structure of cobalt foam is beneficial to the rapid transfer of gas and exchange of reactive substances. (4) The shell structure of the hydroxide helps to prevent the loss of internal phosphates, thus endowing the long-term stability and high activity of catalyst.

In summary, we have developed a simple, fast and practical strategy to synthesize CoRuOH/Co_2P/CF electrocatalysts with high HER activity in alkaline solution. Benefiting from the combination of molten salt and rapid hydrolysis (30 s), the prepared catalyst possesses double active sites for HER. The OH^- obtained by surface hydrolysis of Co_2P activates the formation of thin CoRuOH layer. The synergistic effect of CoRuOH/Co_2P leads to the water dissociation and the rapid hydrogen adsorption-desorption, which improves HER performance in alkaline solution. When measured in 1.0 mol/L KOH at 25 °C, the obtained CoRuOH/Co_2P/CF only needs

low overpotential of 81 mV to reach 100 mA/cm^2. Even at higher current densities than those for industrial applications, it can also operate stably for at least 100 h. When coupled with a common OER catalyst (NiFe-LDH/IF), it still presents a low cell voltage (1.77 V) for alkaline water electrolysis to achieve the current density of 1000 mA/cm^2 with outstanding stability, which makes it a great potential for large-scale production of hydrogen. Therefore, this work opens up a new avenue for enhancing HER performance of transition metal-based phosphates for water splitting or other related energy fields.

Declaration of competing interest

The authors declare that they have no known competing financial interests or personal relationships that could have appeared to influence the work reported in this paper.

Acknowledgment

This work is financially supported by the National Natural Science Foundation of China (Nos. 52174283 and 52274308).

Supplementary materials

Supplementary material associated with this article can be found, in the online version, at doi:10.1016/j.cclet.2023.109221.

References

[1] B. Wulan, L. Zhao, D. Tan, et al., Adv. Energy Mater. 12 (2022) 2103960.
[2] X. Cao, L. Zhao, B. Wulan, et al., Angew. Chem. Int. Ed. 61 (2022) e202113918.
[3] F.M. Zhang, Y.L. Liu, F. Yu, et al., ACS Nano 17 (2023) 1681.
[4] J.Y. Zhang, H. Wang, Y. Tian, et al., Angew. Chem. Int. Ed. 57 (2018) 7649–7653.
[5] B. Dong, Y.N. Zhou, J.C. Zhou, et al., Fuel 324 (2022) 124343.
[6] X. Zhou, Y.X. Mo, F. Yu, et al., Adv. Funct. Mater. 33 (2023) 2209465.
[7] K. Chen, K. Mao, Y. Bai, et al., Chin. Chem. Lett. 33 (2022) 452–456.
[8] J. Chen, Y. Ha, R. Wang, et al., Nano-Micro Lett. 14 (2022) 186.
[9] J. Xu, M. Zhong, N. Song, C. Wang, X. Lu, Chin. Chem. Lett. 34 (2023) 107359.
[10] Z. Li, W. Wang, Q. Qian, et al., eScience 2 (2022) 416–427.
[11] X. Shang, K.L. Yan, Z.Z. Liu, et al., Appl. Surf. Sci. 402 (2017) 120–128.
[12] Z. Li, Y. Yue, J. Peng, Z. Luo, Chin. Chem. Lett. 34 (2023) 107119.
[13] G. Fu, X. Kang, Y. Zhang, et al., Nano-Micro Lett. 14 (2022) 200.
[14] X.Y. Zhang, Y.R. Zhu, Y. Chen, et al., Chem. Eng. J. 399 (2020) 125831.
[15] Y. Jiang, Y. Li, Y. Jiang, et al., Chin. Chem. Lett. 33 (2022) 4003–4007.
[16] B. Dong, J.Y. Xie, N. Wang, et al., Renew. Energy 157 (2020) 415–423.
[17] C. Wei, Y. Sun, G.G. Scherer, et al., J. Am. Chem. Soc. 142 (2020) 7765–7775.
[18] J.Q. Chi, J.Y. Xie, W.W. Zhang, et al., ACS Appl. Mater. Interfaces 11 (2019) 4047–4056.
[19] H. Zhou, F. Yu, Q. Zhu, et al., Energy Environ. Sci. 11 (2018) 2858–2864.
[20] M. Zheng, K. Guo, W.J. Jiang, et al., Appl. Catal. B: Environ. 244 (2019) 1004–1012.
[21] H. Wang, H.W. Lee, Y. Deng, et al., Nat. Commun. 6 (2015) 7261.
[22] T. Wang, X. Cao, L. Jiao, eScience 1 (2021) 69–74.
[23] J. Chen, J. Huang, H. Wang, et al., Chin. Chem. Lett. 33 (2022) 3752–3756.
[24] Q. Li, Y. Wang, J. Zeng, et al., Chin. Chem. Lett. 32 (2021) 3355–3358.
[25] Y. Zhang, L. Gao, E.J.M. Hensen, J.P. Hofmann, ACS Energy Lett. 3 (2018) 1360–1365.
[26] J. Jiang, F. Li, H. Su, et al., Chin. Chem. Lett. 33 (2022) 4367–4374.
[27] J.Q. Zhang, X. Shang, H. Ren, et al., Adv. Mater. 31 (2019) 1905107.
[28] Q. Zhang, S. Jiao, B. Wang, et al., Int. J. Hydrog. Energy 46 (2021) 26329–26339.
[29] Y. Wei, X. Zhang, Z. Wang, et al., Chin. Chem. Lett. 32 (2021) 119–124.
[30] J. Yu, W. Yu, B. Chang, et al., Chin. Chem. Lett. 33 (2022) 3231–3235.
[31] J.Y. Xie, H.Y. Zhao, Y.W. Dong, et al., Chin. J. Struct. Chem. 41 (2022) 2207053–2207058.
[32] L. Fu, F. Yang, Y. Hu, et al., Sci Bull. 65 (2020) 1735–1742.
[33] X. Guo, X. Wan, Q. Liu, et al., eScience 2 (2022) 304–310.
[34] H. Xu, J. Zhu, P. Wang, et al., J. Mater. Chem. A 9 (2021) 24677–24685.
[35] T. Liu, P. Li, N. Yao, et al., Angew. Chem. Int. Ed. 58 (2019) 4976–4984.
[36] Y.R. Liu, W.H. Hu, G.Q. Han, et al., Electrochim. Acta 220 (2016) 98–106.
[37] Q. Zhou, Q. Bian, L. Liao, et al., Chin. Chem. Lett. 34 (2023) 107248.
[38] S.W. Jang, S. Dutta, A. Kumar, et al., ACS Nano 14 (2020) 10578–10588.
[39] Y. Zhao, X. Wang, Z. Li, et al., Chin. Chem. Lett. 33 (2022) 1065–1069.
[40] X.Y. Zhang, B.Y. Guo, F.T. Li, et al., Int. J. Hydrog. Energy 44 (2019) 21683–21691.
[41] S. Yuan, J. Peng, B. Cai, et al., Nat. Mater. 21 (2022) 673–680.
[42] K.L. Zhou, C. Wang, Z. Wang, et al., Energy Environ. Sci. 13 (2020) 3082–3092.
[43] F. Zhan, Q. Wang, Y. Li, et al., Inorg. Chem. 57 (2018) 5791–5800.
[44] Y. Liu, S. He, F. Zhan, et al., J. Electrochem. Soc. 167 (2020) 146509.
[45] Y. Men, Y. Tan, P. Li, et al., Appl. Catal. B Environ. 284 (2021) 119718.
[46] Y. Tang, Q. Liu, L. Dong, H.B. Wu, X.Y. Yu, Appl. Catal. B: Environ. 266 (2020) 118627.
[47] C.X. Zhao, B.Q. Li, M. Zhao, et al., Energy Environ. Sci. 13 (2020) 1711–1716.
[48] D. Zhou, S. Wang, Y. Jia, et al., Angew. Chem. Int. Ed. 58 (2019) 736–740.